Advances in Difference Equations
a SpringerOpen Journal

RESEARCH **Open Access**

# Bifurcation, chaos analysis and control in a discrete-time predator–prey system

Weiyi Liu[1*] and Donghan Cai[1]

*Correspondence:
weiyiliu@whu.edu.cn
[1]School of Mathematics and Statistics, Wuhan University, Wuhan, China

**Abstract**

The dynamical behavior of a discrete-time predator–prey model with modified Leslie–Gower and Holling's type II schemes is investigated on the basis of the normal form method as well as bifurcation and chaos theory. The existence and stability of fixed points for the model are discussed. It is showed that under certain conditions, the system undergoes a Neimark–Sacker bifurcation when bifurcation parameter passes a critical value, and a closed invariant curve arises from a fixed point. Chaos in the sense of Marotto is also verified by both analytical and numerical methods. Furthermore, to delay or eliminate the bifurcation and chaos phenomena that exist objectively in this system, two control strategies are designed, respectively. Numerical simulations are presented not only to validate analytical results but also to show the complicated dynamical behavior.

**MSC:** Primary 37N25; secondary 34H10; 34H15; 34H20; 37M20; 39A28

**Keywords:** Predator–prey model; Local stability; Neimark–Sacker bifurcation; Marotto's chaos; Bifurcation control; Chaos control

## 1 Introduction

Predation is a common and very important species interaction in many biological systems. Mathematical models are useful tools to understand and analyze the dynamical behavior of the predator–prey system, among which the Lotka–Volterra model is the oldest and the best known representative. However, this model proved to be overly simplistic and lacking in certain biological features [1]. The famous Leslie–Gower model, one of the many modified Lotka–Volterra models, is based on the assumption that reduction in a predator population has a reciprocal relationship with per capita availability of its preferred food. Indeed, Leslie and Gower [2] introduced a predator–prey model as follows:

$$\begin{cases} \frac{\mathrm{d}H}{\mathrm{d}T} = (a_1 - b_1 H - b_2 P)H, \\ \frac{\mathrm{d}P}{\mathrm{d}T} = a_2 P(1 - \frac{P}{\epsilon H}). \end{cases}$$

Let us mention that the first equation of system is standard. By contrast, the second equation is absolutely not standard and known as classical Leslie–Gower formulation. They stress the fact that there are upper limits to the rates of increase of both prey $H$ and predator $P$, which are not recognized in the Lotka–Volterra model. In the Leslie–Gower formulation, the growth of the predator population is taken as logistic type, i.e., $\frac{\mathrm{d}P}{\mathrm{d}T} = a_2 P(1 - \frac{P}{K})$, where the measures of the environmental carrying capacity $K$ is assumed to be proportional to the prey abundance, that is, $K = \epsilon H$, $\epsilon > 0$ is the conversion factor of prey into predator. The term $\frac{P}{\epsilon H}$ is sometimes called the Leslie–Gower term.

In [3] Aziz-Alaoui and Daher Okiye proposed a predator–prey model that incorporates the Holling's type II functional response and a modified Leslie–Gower term, which is described by the Kolmogorov type [4] autonomous bidimensional differential equations system:

$$\begin{cases} \frac{\mathrm{d}H}{\mathrm{d}T} = (a_1 - b_1 H - \frac{c_1 P}{H+e_1})H, \\ \frac{\mathrm{d}P}{\mathrm{d}T} = (a_2 - \frac{c_2 P}{H+e_2})P, \end{cases} \tag{1.1}$$

with $H(0) \geq 0$ and $P(0) \geq 0$, where $H = H(T)$ and $P = P(T)$ represent the population densities of the prey species and the predator species at time $T$, respectively. The predator consumes the prey by a Holling's type II functional response $\frac{c_1 H}{H+e_1}$. However, the predator does not follow the "mass conservation" principle, but one introduces a modified Leslie–Gower term $\frac{c_2 P}{H+e_2}$. This modification prevents the extinction of predator population in the absence of prey [5, 6]. $a_i$, $c_i$, $e_i$, $i = 1, 2$ and $b_1$ are model parameters and are all positive values, having the following biological meanings:

- $a_1$ and $a_2$ are the natural growth rates of the prey species and the predator species, respectively.
- $b_1$ measures the strength of competition among individuals of the prey species.
- $c_1$ is the maximum value of the per capita reduction of the prey species due to the predator species, $c_2$ has a similar meaning to $c_1$.
- $e_1$ and $e_2$ are the extent to which the environment provides protection to the prey species and the predator species, respectively.

At present, this model has been successfully studied by some authors (cf. [3, 7–9]) and the references therein. Moreover, on the basis of the model system (1.1), many human nature factors are taken into account, such as time delay [10], impulsive effect [11], white noise [12]. Nevertheless, the previous work for this model is mainly concentrated on stability aspect. In recent years experimental and numerical studies have shown that chaos is a widespread phenomenon throughout the biological hierarchy ranging from simple enzyme reactions to ecosystems [13]. On the chaos and bifurcations analysis in nonlinear systems, some interesting results are reported in 2018 (cf. [14–18]). Furthermore, bifurcation and chaos have always been regarded as unfavorable phenomenon in biology. In general, bifurcation is often a precursor to chaos, and chaos can cause the population to run a higher risk of extinction due to the unpredictability, so they are harmful for the breeding of biological population [19]. However, in some existing literature about biological systems [20–22], only the phenomena of bifurcation and chaos were presented. But, to the best of our knowledge, there has been much less work on the problem of bifurcation and chaos control in biological systems. The above-mentioned challenges inspire us to investigate the bifurcation and chaos behavior of this model in the present study. We not only give the theoretical analysis of objectively existing bifurcation and chaos phenomena for this biological system, but also we try to design two control strategies to delay the appearance of bifurcation and stabilize chaotic orbit if system is chaotic, respectively. Our work can be considered as the continuation and development of the work in [3], and the control methods in this paper can be applicable for [20–22] etc.

Many differential equations cannot be solved using symbolic computation ("analysis"). For practical purposes, people sometimes construct difference equation to approximate differential equation so that they can write code to solve differential equation numerically. Moreover, while continuous models have been successfully applied in a variety of situations, one fundamental assumption is that the species in question has continuous, overlapping generations. However, it is observed in nature that many species do not possess this quality. For example, some anadromous fishes, such as salmon, have annual spawning seasons, with births taking place at the same time every year. Many insects breed and die before the next generation emerges, often having overwintered as eggs, larvae or pupae. Annual plant species also set seed and die before the next generation germinates. Populations with this characteristic of non-overlapping generations are much better described by discrete-time (difference equations) model than continuous equations (Hu et al., [23]). In addition, the earlier work [24, 25] showed that the discrete dynamics of the one-dimensional logistic map can produce a much richer set of patterns than those observed in continuous-time model. Therefore, in this paper, we work under a different perspective, where we will focus on the difference scheme of Eq. (1.1).

First, to reduce the arising complexity in the dynamical analysis and interpretation of results, simple changes in variables and parameters are introduced for.

$$t = a_1 T, \qquad u(t) = H(T), \qquad v(t) = \frac{c_2}{a_2} P(T), \qquad \beta = \frac{b_1}{a_1}, \qquad m = \frac{a_2 c_1}{a_1 c_2}, \qquad s = \frac{a_2}{a_1}.$$

Using the above transformation, (1.1) takes the form

$$\begin{cases} \frac{\mathrm{d}u}{\mathrm{d}t} = u(1 - \beta u) - \frac{muv}{u+e_1}, \\ \frac{\mathrm{d}v}{\mathrm{d}t} = sv(1 - \frac{v}{u+e_2}). \end{cases} \tag{1.2}$$

In order to derive a discrete form of Eq. (1.2), consider the approximation algorithm, attributed to Euler, as follows:

$$\frac{\mathrm{d}u}{\mathrm{d}t} \approx \frac{u_{n+1} - u_n}{\Delta t}, \qquad \frac{\mathrm{d}v}{\mathrm{d}t} \approx \frac{v_{n+1} - v_n}{\Delta t},$$

where $u_n$ (or $v_n$) and $u_{n+1}$ (or $v_{n+1}$) are consecutive points, separated by a time step $\Delta t$. Now, applying Euler's method with step size 1 to (1.2) gives the following:

$$\begin{cases} u_{n+1} = u_n + u_n(1 - \beta u_n) - \frac{m u_n v_n}{u_n + e_1}, \\ v_{n+1} = v_n + s v_n(1 - \frac{v_n}{u_n + e_2}), \end{cases} \tag{1.3}$$

which defines a two-dimensional discrete-time dynamical system

$$\begin{pmatrix} u \\ v \end{pmatrix} \mapsto \begin{pmatrix} u + u(1 - \beta u) - \frac{muv}{u+e_1} \\ v + sv(1 - \frac{v}{u+e_2}) \end{pmatrix}. \tag{1.4}$$

In the present paper, we shall consider how the natural growth rates of predator and prey affect the dynamical behavior of model system (1.4). The main purpose of the paper is to show that (1.4) possesses the Neimark–Sacker bifurcation and chaos in the sense of

Marotto. Especially, using a hybrid control strategy, the bifurcation threshold value can be raised to a prior setting one so that bifurcation phenomenon be delayed or eliminated in practice. Additionally, if the system is in chaotic state under certain parametric conditions, the chaos orbits can be stabilized to an unstable fixed point by a controller. Numerical simulations are presented to illustrate the analytic results, and to obtain even more dynamical behavior of (1.4), including diagrams for bifurcation, time series plots, phase portraits, strange attractors and the largest Lyapunov exponents.

The paper is organized as follows. In Sect. 2 we discuss the existence and stability of fixed points for model system (1.4). In Sect. 3, we give some details as regards bifurcation analysis of (1.4) as well as accurate control of bifurcation phenomenon. In Sect. 4 conditions on the existence of chaos in the sense of Marotto are given, and some control techniques have been used to stabilize chaos orbits. Finally, some conclusions close the paper in Sect. 5.

## 2 The existence and stability of fixed points

### 2.1 Biomass equilibria and their existence

The model system (1.4) possesses the following three fixed points:

(i) The trivial fixed point $E_0 = (0, 0)$.

(ii) The predator free axial fixed point $E_1 = (\frac{1}{\beta}, 0)$. The biological interpretation of this boundary fixed point is that the prey population reaches in the carrying capacity in the absence of predators.

(iii) The steady state of coexistence (interior fixed point) $E_2 = (\eta, \eta + e_2)$, if

(H1) $me_2 < e_1$

holds, where

$$\eta = \frac{\sqrt{(\beta e_1 + m - 1)^2 - 4\beta(me_2 - e_1)} - (\beta e_1 + m - 1)}{2\beta},$$

i.e., $u = \eta$, $v = \eta + e_2$, denoted by $u^*$, $v^*$, respectively, is the positive root of the following equations:

$$\begin{cases} u(1 - \beta u) - \frac{muv}{u+e_1} = 0, \\ sv(1 - \frac{v}{u+e_2}) = 0. \end{cases}$$

### 2.2 Dynamical behavior: stability analysis

In this subsection, we deal with local stability of (1.4). Let $J_k$ denote the Jacobian matrix of (1.4) at the fixed point $E_k$, $k = 0, 1, 2$, and let $\lambda_1$ and $\lambda_2$ be the two eigenvalues of $J_k$. We first recall some definitions of topological types for a fixed point.

**Definition 2.1** $E_k$ is called a

(i) hyperbolic fixed point, if $|\lambda_1| \neq 1$ and $|\lambda_2| \neq 1$;

(ii) nonhyperbolic fixed point, if $|\lambda_1| = 1$ or $|\lambda_2| = 1$.

**Definition 2.2** If $E_k$ is a hyperbolic fixed point, then it is called a

(i) sink, if $|\lambda_1| < 1$ and $|\lambda_2| < 1$;

(ii) source, if $|\lambda_1| > 1$ and $|\lambda_2| > 1$;

(iii) saddle, if $\lambda_{1,2}$ are real with $|\lambda_1| < 1$ and $|\lambda_2| > 1$ (or $|\lambda_1| > 1$ and $|\lambda_2| < 1$).

*2.2.1 The behavior of the model system (1.4) around $E_0$*

The variational matrix $J_0$, in the small neighborhood of trivial fixed point $E_0$, is given by

$$J_0 = \begin{pmatrix} 2 & 0 \\ 0 & 1+s \end{pmatrix}.$$

We observe that $J_0$, the jacobian matrix of (1.4) at fixed point $E_0$, has eigenvalues 2 and $1+s$. Therefore, (1.4) is always unstable around $E_0$, which is, in fact, a source.

*2.2.2 The behavior of the model system (1.4) around $E_1$*

The variational matrix $J_1$ in the small neighborhood of fixed point $E_1$ is

$$J_1 = \begin{pmatrix} 0 & -\frac{m}{1+\beta e_1} \\ 0 & 1+s \end{pmatrix}.$$

Eigenvalues of variational matrix $J_1$ at the fixed point $E_1$ are 0 and $1+s$. Hence, (1.4) is unstable around $E_1$, which is in fact a saddle.

*2.2.3 The behavior of the model system (1.4) around $E_2$*

The Jacobian matrix of map (1.4) at any point $(u,v)$, denoted by $J_{(u,v)}$, is given by

$$J_{(u,v)} = \begin{pmatrix} 2-2\beta u - \frac{mv}{u+e_1} + \frac{muv}{(u+e_1)^2} & -\frac{mu}{u+e_1} \\ \frac{sv^2}{(u+e_2)^2} & 1+s(1-\frac{v}{u+e_2}) - \frac{sv}{u+e_2} \end{pmatrix},$$

and the characteristic equation associated to $J_{(u,v)}$ is

$$\Phi(\lambda) = \lambda^2 + B\lambda + C = 0,$$

where

$$\begin{cases} B(u,v) = -3 + 2\beta u + \frac{mv}{u+e_1} - \frac{muv}{(u+e_1)^2} - s(1-\frac{v}{u+e_2}) + \frac{sv}{u+e_2}, \\ C(u,v) = (2-2\beta u - \frac{mv}{x+e_1} + \frac{muv}{(u+e_1)^2})(1+s(1-\frac{v}{u+e_2}) - \frac{sv}{u+e_2}) \\ \qquad + \frac{musv^2}{(u+e_1)(u+e_2)^2}. \end{cases} \tag{2.1}$$

Hence,

$$J_2 = \begin{pmatrix} 2-2\beta\eta - \frac{m(\eta+e_2)}{\eta+e_1} + \frac{m\eta(\eta+e_2)}{(\eta+e_1)^2} & -\frac{m\eta}{\eta+e_1} \\ s & 1-s \end{pmatrix},$$

and the characteristic equation of $J_2$ can be written as

$$\lambda^2 - (s_0 + 1 - s)\lambda + s_0(1-s) - bs = 0,$$

where

$$s_0 = 2 - 2\beta\eta - \frac{m(\eta+e_2)}{\eta+e_1} + \frac{m\eta(\eta+e_2)}{(\eta+e_1)^2},$$

$$b = -\frac{m\eta}{\eta+e_1}.$$

In order to discuss the stability of the fixed points, we also need the following lemma, which can be easily proved by the relations between roots and coefficients of a quadratic equation [26].

**Lemma 2.1** *Suppose that* $\Phi(1) > 0$. *Then*

(i) $|\lambda_1| < 1$ *and* $|\lambda_2| < 1$ *iff* $\Phi(-1) > 0$ *and* $C < 1$;
(ii) $|\lambda_1| > 1$ *and* $|\lambda_2| > 1$ *iff* $\Phi(-1) > 0$ *and* $C > 1$;
(iii) $|\lambda_1| < 1$ *and* $|\lambda_2| > 1$ (*or* $|\lambda_1| > 1$ *and* $|\lambda_2| < 1$) *iff* $\Phi(-1) < 0$;
(iv) $\lambda_1$ *and* $\lambda_2$ *are complex and* $|\lambda_1| = |\lambda_2| = 1$ *iff* $B^2 - 4C < 0$ *and* $C = 1$;
(v) $\lambda_1 = -1$ *and* $|\lambda_2| \neq 1$ *iff* $\Phi(-1) = 0$ *and* $B \neq 0, 2$.

Using Definition 2.2 and Lemma 2.1, we obtain the following results.

**Theorem 2.1** *Assume that* (H1) *holds. Then* $E_2$ *is*

(i) *a sink if one of the following conditions holds*:
 (i.1) $0 < s_0 + b < 1$ *and* $\frac{s_0-1}{s_0+b} < s < \frac{2(1+s_0)}{s_0+b+1}$;
 (i.2) $-1 < s_0 + b < 0$ *and* $s < \min\{\frac{2(1+s_0)}{s_0+b+1}, \frac{s_0-1}{s_0+b}\}$;
 (i.3) $s_0 + b < -1$ *and* $\frac{s_0-1}{s_0+b} > s > \frac{2(1+s_0)}{s_0+b+1}$;
(ii) *a source if one of the following conditions holds*:
 (ii.1) $0 < s_0 + b < 1$ *and* $s < \min\{\frac{2(1+s_0)}{s_0+b+1}, \frac{s_0-1}{s_0+b}\}$;
 (ii.2) $-1 < s_0 + b < 0$ *and* $\frac{s_0-1}{s_0+b} < s < \frac{2(1+s_0)}{s_0+b+1}$;
 (ii.3) $s_0 + b < -1$ *and* $s > \max\{\frac{2(1+s_0)}{s_0+b+1}, \frac{s_0-1}{s_0+b}\}$;
(iii) *a saddle if one of the following conditions holds*:
 (iii.1) $-1 < s_0 + b < 1$ *and* $s > \frac{2(1+s_0)}{s_0+b+1}$;
 (iii.2) $s_0 + b < -1$ *and* $s < \frac{2(1+s_0)}{s_0+b+1}$;
(iv) *nonhyperbolic if one of the following conditions holds*:
 (iv.1) $s_0 + b = 1$;
 (iv.2) $s_0 + b \neq -1$, *and* $s = \frac{2(1+s_0)}{s_0+b+1}$;
 (iv.3) $s_0 + b \neq 0$, $s = \frac{s_0-1}{s_0+b}$ *and* $(s_0 + 1 - s)^2 < 4(s_0(1 - s) - bs)$.

## 3 Neimark–Sacker bifurcation analysis and control

If (iv.3) of Theorem 2.1 holds, we find that the eigenvalues at $E_2$ are a pair of conjugate complex numbers with modulus 1. Let

$$NS = \left\{(m, \beta, e_1, e_2, s) \,\middle|\, s = \frac{s_0 - 1}{s_0 + b}, s \neq s_0 + 3, s_0 - 1, s_0 + b \neq 0, m, \beta, e_1, e_2, s > 0\right\}.$$

Now we investigate Neimark–Sacker bifurcation at $E_2$ if parameters $(m, \beta, e_1, e_2, s)$ vary in a small neighborhood of the set $NS$.

### 3.1 Neimark–Sacker bifurcation analysis

Taking parameters $(m, \beta, e_1, e_2, s)$ arbitrarily from $NS$. Map (1.4) has an interior fixed point $E_2$, at which eigenvalues $\lambda_1$, $\lambda_2$ satisfy $|\lambda_1| = |\lambda_2| = 1$.

In order to transform $E_2$ into the origin, let $x = u - u^*$, $y = v - v^*$, Eq. (1.3) becomes

$$\begin{cases} x_{n+1} = x_n + (x_n + u^*)(1 - \beta(x_n + u^*)) - \frac{m(x_n+u^*)(y_n+v^*)}{x_n+u^*+e_1}, \\ y_{n+1} = y_n + s(y_n + v^*)(1 - \frac{y_n+v^*}{x_n+u^*+e_2}), \end{cases}$$

or in map form

$$\begin{pmatrix} x \\ y \end{pmatrix} \mapsto \begin{pmatrix} x + (x+u^*)(1-\beta(x+u^*)) - \frac{m(x+u^*)(y+v^*)}{x+u^*+e_1} \\ x + s(y+v^*)(1-\frac{y+v^*}{x+u^*+e_2}) \end{pmatrix}. \tag{3.1}$$

Since $(m,\beta,e_1,e_2,s) \in NS$, we find $s = \frac{s_0-1}{s_0+b}$, denoted by $s_1$. Choosing $s^*$ as bifurcation parameter, we consider a perturbation of map (3.1):

$$\begin{pmatrix} x \\ y \end{pmatrix} \mapsto \begin{pmatrix} x + (x+u^*)(1-\beta(x+u^*)) - \frac{m(x+u^*)(y+v^*)}{x+u^*+e_1} \\ y + (s_1+s^*)(y+v^*)(1-\frac{y+v^*}{x+u^*+e_2}) \end{pmatrix}, \tag{3.2}$$

where $|s^*| \ll 1$ is a small parameter. In the following, we derive the Taylor series expansion of the right-hand side of (3.2) at the origin to order 3, that is,

$$\begin{pmatrix} x \\ y \end{pmatrix} \mapsto \begin{pmatrix} a_1x + a_2y + a_{11}x^2 + a_{12}xy + a_{111}x^3 + a_{112}x^2y + O((|x|+|y|)^4) \\ b_1x + b_2y + b_{11}x^2 + b_{12}xy + b_{22}y^2 + b_{111}x^3 + b_{112}x^2y \\ + b_{122}xy^2 + O((|x|+|y|)^4) \end{pmatrix}, \tag{3.3}$$

where

$$\begin{aligned}
&a_1 = 2 - 2\beta u^* - \frac{mv^*}{u^*+e_1} + \frac{mu^*v^*}{(u^*+e_1)^2}, \qquad a_2 = -\frac{mu^*}{u^*+e_1}, \\
&a_{11} = -\beta + \frac{mv^*}{(u^*+e_1)^2} - \frac{mu^*v^*}{(u^*+e_1)^3}, \qquad a_{12} = -\frac{m}{u^*+e_1} + \frac{mu^*}{(u^*+e_1)^2}, \\
&a_{111} = -\frac{mv^*}{(u^*+e_1)^3} + \frac{mu^*v^*}{(u^*+e_1)^4}, \qquad a_{112} = \frac{m}{(u^*+e_1)^2} - \frac{mu^*}{(u^*+e_1)^3}, \\
&b_1 = s_1 + s^*, \qquad b_2 = 1 - s_1 - s^*, \qquad b_{11} = -\frac{s_1+s^*}{u^*+e_2}, \qquad b_{12} = \frac{2(s_1+s^*)}{u^*+e_2}, \\
&b_{22} = -\frac{s_1+s^*}{u^*+e_2}, \qquad b_{111} = \frac{s_1+s^*}{(u^*+e_2)^2}, \qquad b_{112} = -\frac{2(s_1+s^*)}{(u^*+e_2)^2}, \\
&b_{122} = \frac{s_1+s^*}{(u^*+e_2)^2}.
\end{aligned}$$

Note that the characteristic equation associated with map (3.2) at $E_2$ is given by

$$\lambda^2 + B(s^*)\lambda + C(s^*) = 0,$$

where

$$\begin{aligned}
&B(s^*) = -s_0 - 1 + (s_1 + s^*), \\
&C(s^*) = s_0(1 - (s_1 + s^*)) - (s_1 + s^*)b,
\end{aligned}$$

thus, if $s^*$ varies in a small neighborhood of the origin, the roots of characteristic equation are

$$\begin{aligned}
\lambda_{1,2} = {} & \frac{(s_0 + 1 - (s_1 + s^*))}{2} \\
& \pm \frac{\mathrm{i}\sqrt{4(s_0(1-(s_1+s^*)) - (s_1+s^*)b) - (s_0 + 1 - (s_1+s^*))^2}}{2},
\end{aligned}$$

with

$$|\lambda_{1,2}| = \sqrt{C(s^*)}, \qquad \alpha = \frac{\mathrm{d}|\lambda_{1,2}|}{\mathrm{d}s^*}\bigg|_{s^*=0} = -\frac{1}{2}(s_0+b) \neq 0.$$

In addition, it is required that $\lambda_{1,2}^i \neq 1$ for $i \neq 1,2,3,4$, if $s^* = 0$. It is equivalent to $B(0) \neq -2,0,1,2$. Since $(m,\beta,e_1,e_2,s_1) \in NS$, one would just need to require $B(0) \neq 0,1$, which leads to

(H2) $s_1 \neq 1+s_0, 2+s_0$.

Constructing an invertible matrix

$$T = \begin{pmatrix} a_2 & 0 \\ \sigma - a_1 & -\omega \end{pmatrix},$$

where $\sigma = -\frac{B(0)}{2}$, $\omega = \frac{\sqrt{4C(0)-B^2(0)}}{2}$, and using the translation

$$\begin{pmatrix} x \\ y \end{pmatrix} = T\begin{pmatrix} \overline{x} \\ \overline{y} \end{pmatrix},$$

then the map (3.3) can be changed into

$$\begin{pmatrix} \overline{x} \\ \overline{y} \end{pmatrix} \mapsto \begin{pmatrix} \sigma & -\omega \\ \omega & \sigma \end{pmatrix}\begin{pmatrix} \overline{x} \\ \overline{y} \end{pmatrix} + \begin{pmatrix} \overline{f}_1(\overline{x},\overline{y}) \\ \overline{f}_1(\overline{x},\overline{y}) \end{pmatrix}, \tag{3.4}$$

now with linear part in normal form, where

$$\begin{aligned}
\overline{f}_1(\overline{x},\overline{y}) &= (-a_1a_{12} + a_{11}a_2 + a_{12}\sigma)\overline{x}^2 - a_{12}\omega\overline{xy} + \big(a_{111}a_2^2 + a_{112}a_2\sigma \\
&\quad - a_1a_{112}a_2\big)\overline{x}^3 - a_{112}a_2\omega\overline{x}^2\overline{y} + O\big(\big(|\overline{x}| + |\overline{y}|\big)^4\big), \\
\overline{f}_2(\overline{x},\overline{y}) &= \frac{1}{\omega}\big(a_1{}^2a_{12} - a_1{}^2b_{22} - a_2a_1a_{11} - 2a_1a_{12}\sigma + a_2a_1b_{12} + 2a_1b_{22}\sigma \\
&\quad + a_2a_{11}\sigma + a_{12}\sigma^2 - b_{11}a_2{}^2 - a_2b_{12}\sigma - b_{22}\sigma^2\big)\overline{x}^2 + (a_2b_{12} + 2b_{22}\sigma \\
&\quad - 2a_1b_{22} + a_1a_{12} - a_{12}\sigma)\overline{xy} - \omega b_{22}\overline{y}^2 + \frac{1}{\omega}\big(a_2a_1{}^2a_{112} - a_1{}^2a_2b_{122} \\
&\quad - a_2{}^2a_1a_{111} - 2a_2a_1a_{112}\sigma + a_1a_2{}^2b_{112} + 2a_1a_2b_{122}\sigma + a_2{}^2a_{111}\sigma \\
&\quad + a_2a_{112}\sigma^2 - b_{111}a_2{}^3 - a_2{}^2b_{112}\sigma - a_2b_{122}\sigma^2\big)\overline{x}^3 - \omega a_2b_{122}\overline{xy}^2 \\
&\quad + \big(a_2a_1a_{112} - 2a_1a_2b_{122} - a_2a_{112}\sigma + a_2{}^2b_{112} + 2a_2b_{122}\sigma\big)\overline{x}^2\overline{y} \\
&\quad + O\big(\big(|\overline{x}| + |\overline{y}|\big)^4\big),
\end{aligned}$$

with

$$\begin{aligned}
&\overline{f}_{1\overline{xx}} = -2a_1a_{12} + 2a_{11}a_2 + 2a_{12}\sigma, \qquad \overline{f}_{1\overline{xy}} = -a_{12}\omega, \qquad \overline{f}_{1\overline{yy}} = 0, \\
&\overline{f}_{1\overline{xxx}} = -6a_1a_{112}a_2 + 6a_{111}a_2{}^2 + 6a_{112}a_2\sigma, \qquad \overline{f}_{1\overline{xxy}} = -2a_{112}a_2\omega, \\
&\overline{f}_{1\overline{xyy}} = 0, \qquad \overline{f}_{1\overline{yyx}} = 0, \qquad \overline{f}_{1\overline{yyy}} = 0,
\end{aligned}$$

$$\begin{aligned}
\overline{f}_{2\overline{xx}} &= \frac{1}{\omega}\big(2{a_1}^2a_{12} - 2{a_1}^2b_{22} - 2a_2a_1a_{11} - 4a_1a_{12}\sigma + 2a_1a_2b_{12} \\
&\quad + 4a_1b_{22}\sigma + 2a_2a_{11}\sigma + 2a_{12}\sigma^2 - 2b_{11}{a_2}^2 - 2a_2b_{12}\sigma - 2b_{22}\sigma^2\big), \\
\overline{f}_{2\overline{xy}} &= a_1a_{12} - 2a_1b_{22} - a_{12}\sigma + a_2b_{12} + 2b_{22}\sigma, \qquad \overline{f}_{2\overline{yy}} = -2\omega b_{22}, \\
\overline{f}_{2\overline{xxx}} &= \frac{1}{\omega}\big(6a_2{a_1}^2a_{112} - 6{a_1}^2a_2b_{122} - 6{a_2}^2a_1a_{111} - 12a_2a_1a_{112}\sigma \\
&\quad + 6a_1{a_2}^2b_{112} + 12a_1a_2b_{122}\sigma + 6{a_2}^2a_{111}\sigma + 6a_2a_{112}\sigma^2 - 6b_{111}{a_2}^3 \\
&\quad - 6{a_2}^2b_{112}\sigma - 6a_2b_{122}\sigma^2\big), \\
\overline{f}_{2\overline{xxy}} &= 2a_1a_{112}a_2 - 4a_1a_2b_{122} - 2a_{112}a_2\sigma + 2{a_2}^2b_{112} + 4a_2b_{122}\sigma, \\
\overline{f}_{2\overline{xyy}} &= -2\omega a_2b_{122}, \qquad \overline{f}_{2\overline{yyy}} = 0.
\end{aligned}$$

In order for system (3.4) to undergo a Neimark–Sacker bifurcation at the origin, we require that the following quantity is not zero [25, 27]:

$$L = -\operatorname{Re}\left(\frac{(1-2\lambda)\overline{\lambda}^2}{1-\lambda}\gamma_{20}\gamma_{11}\right) - \frac{1}{2}|\gamma_{11}|^2 - |\gamma_{02}|^2 + \operatorname{Re}(\overline{\lambda}\gamma_{21}), \tag{3.5}$$

where

$$\begin{aligned}
\gamma_{20} &= \frac{(\overline{f}_{1\overline{xx}} - \overline{f}_{1\overline{yy}} + 2\overline{f}_{2\overline{xy}}) + i(\overline{f}_{2\overline{xx}} - \overline{f}_{2\overline{yy}} - 2\overline{f}_{1\overline{xy}})}{8}, \\
\gamma_{11} &= \frac{(\overline{f}_{1\overline{xx}} + \overline{f}_{1\overline{yy}}) + i(\overline{f}_{2\overline{xx}} + \overline{f}_{2\overline{yy}})}{4}, \\
\gamma_{02} &= \frac{(\overline{f}_{1\overline{xx}} - \overline{f}_{1\overline{yy}} - 2\overline{f}_{2\overline{xy}}) + i(\overline{f}_{2\overline{xx}} - \overline{f}_{2\overline{yy}} + 2\overline{f}_{1\overline{xy}})}{8}, \\
\gamma_{21} &= \frac{\overline{f}_{1\overline{xxx}} + \overline{f}_{1\overline{xyy}} + \overline{f}_{2\overline{xxy}} + \overline{f}_{2\overline{yyy}}}{16} + \frac{i(\overline{f}_{2\overline{xxx}} + \overline{f}_{2\overline{xyy}} + \overline{f}_{1\overline{xxy}} + \overline{f}_{1\overline{yyy}})}{16}.
\end{aligned}$$

Summarizing, we have established the following result for Neimark–Sacker bifurcation behavior of the model system (1.4):

**Theorem 3.1** *Assume that conditions* (H1) *and* (H2) *hold. Then if* $L \neq 0$, *the model system* (1.4) *undergoes a Neimark–Sacker bifurcation at fixed point* $E_2$ *when the parameter* $s$ *varies in a small neighborhood of* $s_1$. *Moreover, if* $L < 0$ (*respectively,* $L > 0$), *then an attracting* (*respectively, a repelling*) *closed invariant curve bifurcates form* $E_2$.

*Remark* 3.1 From the biological point of view, an invariant curve bifurcates from a fixed point, which means that the prey and predator can coexist in a stable way and reproduce their densities. The dynamics on the invariant curve may be either periodic or quasi-periodic.

*Example* 3.1 Neimark–Sacker bifurcation.

Parameter values are fixed as $m = 3$, $\beta = 0.2$, $e_1 = 1.2$, $e_2 = 0.3$. Simple calculation yields $E_2 = (0.13236426, 0.43236426)$, $s_1 = 0.09096349222$. When $s = s_1$, the corresponding eigenvalues are $\lambda_{1,2} \approx 0.9896395489 \pm 0.1435742421i$ with $|\lambda_{1,2}| = 1$, and

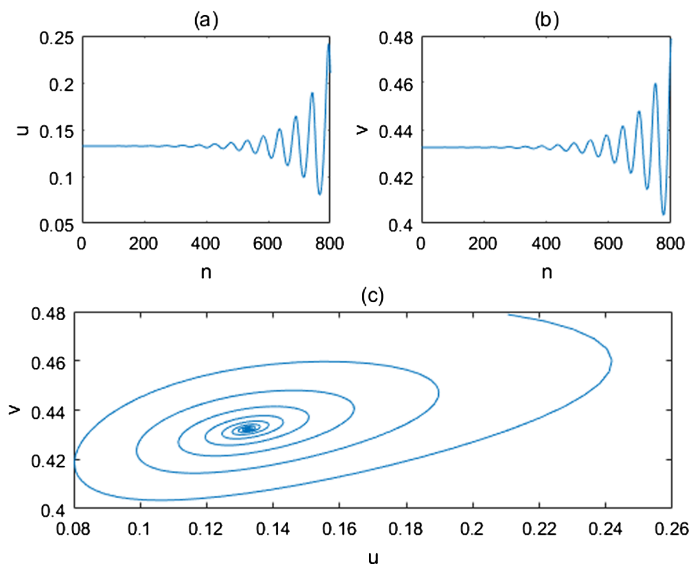


**Figure 1** $s = s_1 - 0.02596349222$, the fixed point (0.13236426, 0.43236426) is unstable

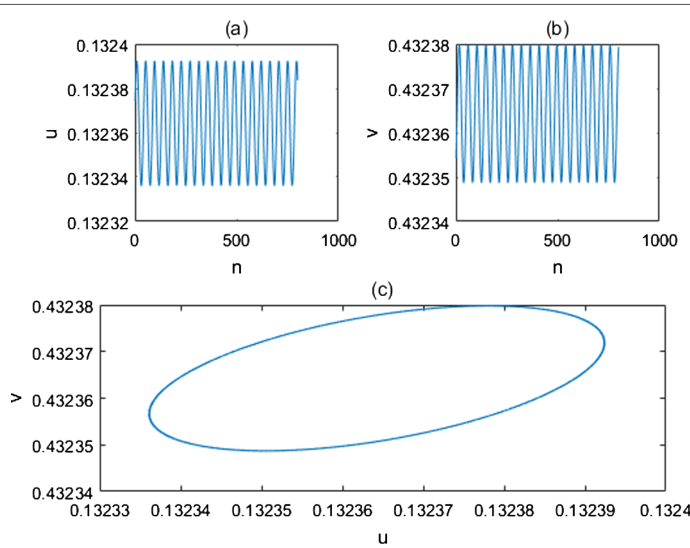


**Figure 2** $s = s_1 + 0.00000650778$ is in a small neighborhood of $s_1 = 0.09096349222$. A repelling closed invariant curve bifurcates from the fixed point (0.13236426, 0.43236426) in the map (1.4) without control

$\alpha = -0.3861031954$. By Theorem 3.1, a Neimark–Sacker bifurcation emerges from $E_2$ at $s = s_1$ with $L = 0.00159198374$. It reveals that the fixed point $E_2$ is unstable for $s = 0.065 < s_1$ (Fig. 1), becomes stable for $s = 0.13 > s_1$ (Fig. 3), and a repelling limit cycle appears around it at $s = 0.09097$ (Fig. 2).

### 3.2 Controlling Neimark–Sacker bifurcation by using a hybrid control strategy

In [28, 29] the authors control the Neimark–Sacker bifurcation using polynomial functions. In [30] Luo and Chen design a hybrid control strategy to control flip bifurcation, and it is shown that the hybrid control strategy is very effective in controlling bifurcations for one-dimensional discrete dynamical systems. In this subsection, we extend the hybrid

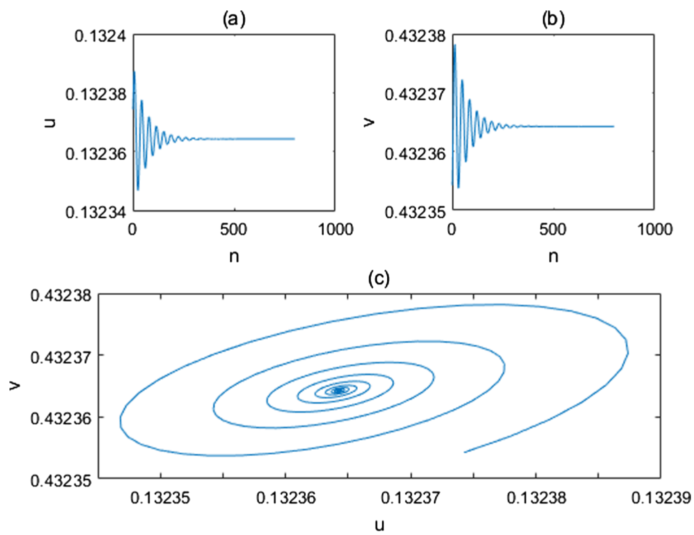


**Figure 3** $s = s_1 + 0.03903650778$, the fixed point (0.13236426, 0.43236426) is stable

control strategy to control Neimark–Sacker bifurcation of model system (1.4) and this can be implemented by means of a biological control [31] or some harvesting procedures [32].

Before beginning our discussion, it is convenient to introduce some notations which will be used frequently from now on:

$$f_1(u,v) = u + u(1-\beta u) - \frac{muv}{u+e_1},$$
$$f_2(u,v) = v + sv\left(1 - \frac{v}{u+e_2}\right),$$
$$F = (f_1, f_2)^{\mathrm{T}},$$
$$z = (u,v)^{\mathrm{T}}.$$

So, the original system (1.4) becomes

$$z_{n+1} = F(z_n). \tag{3.6}$$

Next, we construct the controlled system as follows:

$$z_{n+\kappa} = \gamma F^{\kappa}(z_n) + (1-\gamma)z_n, \tag{3.7}$$

where $\gamma$ is an adjustable parameter with $0 < \gamma < 1$, $\kappa$ is a positive integer, and $F^{\kappa}$ is the $\kappa$th iteration of $F$. Obviously, the controlled system (3.7) degenerates into the original system (3.6) if $\gamma = 1$.

Comparing system (3.6) with (3.7), we have the following result.

**Theorem 3.2** *The controlled system* (3.7) *and the original system* (3.6) *have the same* $\kappa$*-periodic orbit.*

*Remark* 3.2 The control strategy (3.7) is the combination of state feedback and parameter adjustment, and adopts the following issues.

(i) A continuous control scheme if $\kappa = 1$. Namely, controlling fixed points. Control needs to be added for each iteration.

(ii) An impulsive control scheme if $\kappa > 1$. Control is added once only after every $\kappa$th iteration.

Since the aim of this study is to focus on the fixed point bifurcation, we let $\kappa = 1$ in (3.7), which leads to

$$\begin{cases} u_{n+1} = \gamma(u_n + u_n(1-\beta u_n) - \frac{mu_nv_n}{u_n+e_1}) + (1-\gamma)u_n, \\ v_{n+1} = \gamma(v_n + sv_n(1-\frac{v_n}{u_n+e_2})) + (1-\gamma)v_n, \end{cases} \tag{3.8}$$

or in map form

$$\begin{pmatrix} u \\ v \end{pmatrix} \mapsto \begin{pmatrix} \gamma(u + u(1-\beta u) - \frac{muv}{u+e_1}) + (1-\gamma)u \\ \gamma(v + sv(1-\frac{v}{u+e_2})) + (1-\gamma)v \end{pmatrix}.$$

From Theorem 3.2, it follows that systems (3.6) and (3.8) have the same fixed point $E_2$.

In order to check how the implementation of hybrid control strategy works, we have performed the following numerical simulation.

*Example* 3.2 Controlling Neimark–Sacker bifurcation.

Here we will delay the Neimark–Sacker bifurcation of the controlled system (3.8) at $s = 0.12$ (other parameters are the same as given in Example 3.1). The Jacobian matrix at $E_2$ is

$$\bar{J}_2 = \begin{pmatrix} 0.07024259\gamma + 1 & -0.2980361992\gamma \\ 0.12\gamma & -0.12\gamma + 1 \end{pmatrix}.$$

Its corresponding eigenvalue equation is

$$\lambda^2 + (0.04975741\gamma - 2)\lambda + 0.0273352331\gamma^2 - 0.04975741\gamma + 1 = 0. \tag{3.9}$$

With Lemma 2.1, Eq. (3.9) has two conjugate roots with modulus 1 if the following conditions are satisfied:

(i) $1 + (0.04975741\gamma - 2) + 0.0273352331\gamma^2 - 0.04975741\gamma + 1 > 0$;

(ii) $0.0273352331\gamma^2 - 0.04975741\gamma + 1 = 1$;

(iii) $(0.04975741\gamma - 2)^2 - 4(0.0273352331\gamma^2 - 0.04975741\gamma + 1) < 0$.

Choosing $\gamma = 1.820266538$, the conditions (i)–(iii) are satisfied. Thus fixing $\gamma = 1.820266538$, the eigenvalue equation (3.9) becomes $\lambda^2 - 1.909428251\lambda + 1 = 0$. When $s = 0.12$, we have $\lambda_{1,2} = 0.9547141255 \pm 0.2975246856i$ with $|\lambda_{1,2}| = 1$, $\lambda_{1,2}^i \neq 1$ $(i = 1, 2, 3, 4)$ and $\frac{d|\lambda_{1,2}(s)|}{ds}|_{s=0.12} = -1.450849109 \neq 0$. So the controlled system (3.8) undergoes a Neimark–Sacker bifurcation at $s = 0.12$.

On the basis of the above work, we choose $\gamma = 1.820266538$, $s = 0.12$, the controlled system (3.8) becomes

$$\begin{cases} u_{n+1} = 2.820266538u_n - 0.3640533076u_n^2 - \frac{5.460799614u_n v_n}{u_n+1.2}, \\ v_{n+1} = 1.218431985v_n - \frac{0.2184319846v_n^2}{u_n+0.3}. \end{cases} \tag{3.10}$$

Now, we calculate $L$ according to Eq. (3.5). We first turn the fixed point $E_2$ of controlled system (3.10) into the origin. By the transformation

$$\begin{cases} x_n = u_n - 0.13236426, \\ y_n = v_n - 0.43236426, \end{cases}$$

(3.10) becomes

$$\begin{cases} x_{n+1} = 2.820266538x_n + 0.2409382333 \\ \qquad - 0.3640533076(x_n + 0.13236426)^2 \\ \qquad - \frac{5.460799614(x_n+0.13236426)(y_n+0.43236426)}{x_n+1.33236426}, \\ y_{n+1} = 1.218431985y_n + 0.0944421836 - \frac{0.2184319846(y_n+0.43236426)^2}{x_n+0.43236426}. \end{cases} \tag{3.11}$$

Next, using Taylor's formulation, (3.11) becomes

$$\begin{cases} x_{n+1} = 1.127860237x_n - 0.5425053205y_n \\ \qquad + 0.8338405834x_n^2 - 3.691403651x_n y_n \\ \qquad - 0.8990738696x_n^3 + 2.7705664x_n^2 y_n + O((|x_n| + |y_n|)^4), \\ y_{n+1} = 0.2184319845x_n + 0.7815680158y_n \\ \qquad - 0.5052036089x_n^2 + 1.010407218x_n y_n \\ \qquad - 0.5052036091{y_n}^2 + 1.168467553x_n^3 - 2.336935107x_n^2 y_n \\ \qquad + 1.168467553x_n {y_n}^2 + O((|x_n| + |y_n|)^4). \end{cases} \tag{3.12}$$

Constructing an invertible matrix

$$T = \begin{pmatrix} -0.5425053205 & 0 \\ -0.1731461115 & -0.2975246856 \end{pmatrix},$$

and using the variable transformation

$$\begin{pmatrix} x_n \\ y_n \end{pmatrix} = T \begin{pmatrix} \overline{x}_n \\ \overline{y}_n \end{pmatrix},$$

then the system (3.12) can be transformed into the following form:

$$\begin{pmatrix} \overline{x}_{n+1} \\ \overline{y}_{n+1} \end{pmatrix} = \begin{pmatrix} 0.954714125499998 & -0.297524685599999 \\ 0.297524684260071 & 0.954714127300001 \end{pmatrix} \begin{pmatrix} \overline{x}_n \\ \overline{y}_n \end{pmatrix} \\ + \begin{pmatrix} \overline{f}_1(\overline{x}_n, \overline{y}_n) \\ \overline{f}_2(\overline{x}_n, \overline{y}_n) \end{pmatrix},$$

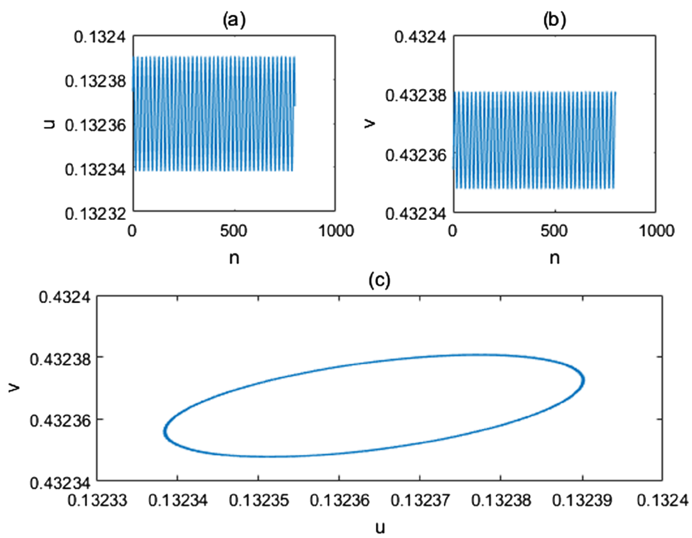


**Figure 4** The repelling closed invariant curve in the controlled map (3.10) for $s = 0.12$

where

$$\begin{aligned}\bar{f}_1(\bar{x}_n,\bar{y}_n) &= 0.18678923522\bar{x}^2 + 1.098283711\overline{xy} - 0.0043615034\bar{x}^3\\ &\quad + 0.44719359\bar{x}^2\bar{y} + O\bigl(\bigl(|\bar{x}_n| + |\bar{y}_n|\bigr)^4\bigr),\\ \bar{f}_2(\bar{x}_n,\bar{y}_n) &= 0.1229517865\bar{x}^2 - 1.012355399\overline{xy} + 0.2932050588\bar{x}^3\\ &\quad - 0.7285202251\bar{x}^2\bar{y} + 0.1503105449\bar{y}^2 + 0.1886008578\overline{xy}^2\\ &\quad + O\bigl(\bigl(|\bar{x}_n| + |\bar{y}_n|\bigr)^4.\end{aligned}$$

With the expression of (3.5), we have $\gamma_{20} = -0.206391541 - 0.2814106174i$, $\gamma_{11} = 0.0933946176 + 0.1366311657i$, $\gamma_{02} = 0.2997861585 + 0.2677312381i$, $\gamma_{21} = -0.09270059512 + 0.1894262031i$, and $L = 0.1558240975 > 0$. The numerical simulation result is shown in Fig. 4, which confirms the existence of a repelling closed orbit in the phase space for $s = 0.12$. On the basis of the above analysis, we deduce that the hybrid control strategy can successfully delay the appearance of the Neimark–Sacker bifurcation.

## 4 Existence of chaos in the sense of Marotto and chaos control

### 4.1 Existence of chaos in the sense of Marotto

In this subsection, with the help of Marotto's theorem [33, 34] we show that map (1.4) exhibits chaotic behavior for specific values of parameters.

Marotto extended Li-York's theorem on chaos from one-dimension to multi-dimension through introducing the notion of snap-back repeller in 1978 [33]. Due to a technical flaw, Marotto redefined a snap-back repeller in 2005 [34]. Marotto's theorem shows that the presence of a snap-back repeller is a sufficient criterion for the existence of chaos. Let us describe the notion of snap-back repeller and Marotto's theorem.

**Definition 4.1** If $\bar{z}$ is a fixed point of $F$ and all the eigenvalues of $DF(\bar{z})$ exceed one in norm, then $\bar{z}$ is called a repelling fixed point of $F$.

**Definition 4.2** Let $\overline{z}$ be a repelling fixed point of $F$. Suppose that there exist a point $z_0 \neq \overline{z}$ in a repelling neighborhood of $\overline{z}$ and an integer $M > 1$, such that $z_M = \overline{z}$ and $\det(DF(z_k)) \neq 0$ for $1 \leq k \leq M$, where $z_k = F^k(z_0)$. Then $\overline{z}$ is called a snap-back repeller of $F$.

**Theorem 4.1** (Marotto's theorem) *If $F$ has a snap-back repeller, then $F$ is chaotic in the following sense: There exist*

(i) *a positive integer $N$, such that $F$ has a point of period $\tau$, for each integer $\tau \geq N$.*

(ii) *a "scrambled set" of $F$, i.e., an uncountable set $S$ containing no periodic points of $F$, such that:*

(ii.1) $F(S) \subset S$;

(ii.2) $\limsup_{x\to\infty} \| F^k(p) - F^k(q) \| > 0$, *for all $p, q \in S$, with $p \neq q$;*

(ii.3) $\limsup_{k\to\infty} \| F^k(p) - F^k(q) \| > 0$, *for all $p \in S$ and periodic point $q$ of $F$;*

(ii.4) *an uncountable subset $S_0$ of $S$, such that* $\limsup_{k\to\infty} \| F^k(p) - F^k(q) \| = 0$, *for every $p, q \in S_0$.*

It is straightforward to see that a snap-back repeller gives rise to an orbit $\{z_k\}_{k=-\infty}^{\infty}$ of $F$ with $z_k = \overline{z}$, for $k \geq M$, and $z_k \to \overline{z}$ as $k \to -\infty$. Roughly speaking, the property of this orbit is analogous to the one for homoclinic orbit. In addition, the map $F$ is locally one-to-one at each point $z_k$. This leads to the trivial transversality, i.e., the unstable manifold $\mathbb{R}^2$ of full dimension intersects transversally the zero-dimensional stable manifold of $\overline{z}$. Therefore, snap-back repeller may be regarded as a special case of a fixed point with a transversal homoclinic orbit [35], which is one of the core concepts in nonlinear dynamics. Especially, homoclinic point, closely related to homoclinic orbit, acts as an organizing center for chaotic motion.

With the definition of snap-back repeller, we adopt the iterative method [36, 37]. We first provide conditions under which the fixed point $\overline{z} = (\overline{u}, \overline{v})$ is a snap-back repeller. Assume that $\mathfrak{B}_r(\overline{z})$ is a certain repelling neighborhood of $\overline{z}$. For all $z = z(u, v) \in \mathfrak{B}_r(\overline{z})$, it is equivalent to the condition

$$\begin{cases} \Phi(1) = 1 + B + C > 0, \\ \Phi(-1) = 1 - B + C > 0, \\ \Phi(0) = C > 1, \end{cases}$$

one has from (2.1)

$$\begin{cases} \Phi(1) = -2 + 2\beta u + \frac{mv}{u+e_1} - \frac{muv}{(u+e_1)^2} - s(1 - \frac{y}{u+e_2}) + \frac{sv}{u+e_2} \\ \qquad + (-2\beta u + 2 - \frac{mv}{u+e_1} + \frac{muv}{(u+e_1)^2})(1 + s(1 - \frac{y}{u+e_2}) - \frac{sy}{u+e_2}) \\ \qquad + \frac{musv^2}{(u+e_1)(u+e_2)^2} > 0, \\ \Phi(-1) = 4 - 2\beta u - \frac{mv}{u+e_1} + \frac{muv}{(u+e_1)^2} + s(1 - \frac{v}{u+e_2}) - \frac{sv}{u+e_2} \\ \qquad + (-2\beta u + 2 - \frac{mv}{u+e_1} + \frac{muv}{(v+e_1)^2})(1 + s(1 - \frac{v}{u+e_2}) - \frac{sv}{u+e_2}) \\ \qquad + \frac{musv^2}{(v+e_1)(v+e_2)^2} > 0, \\ \Phi(0) = (-2\beta u + 2 - \frac{mv}{u+e_1} + \frac{muv}{(u+e_1)^2})(1 + s(1 - \frac{v}{u+e_2}) - \frac{sv}{u+e_2}) \\ \qquad + \frac{uxsv^2}{(u+e_1)(u+e_2)^2} > 1. \end{cases}$$

Let $\Omega_1$, $\Omega_2$ and $\Omega_3$ denote the sets which are defined by aforementioned three inequalities, respectively. We need to find the preimage $z_0$ of $\bar{z}$ in $\mathfrak{B}_r(\bar{z})$, with $z_0 \neq \bar{z}$, $F^M(z_0) = \bar{z}$ and $\det(DF(z_k)) \neq 0$ for $1 \leq k \leq M$ hold. Note that

$$\begin{cases} u_0 + u_0(1 - \beta u_0) - \frac{mu_0v_0}{u_0+e_1} = u_1, \\ v_0 + sv_0(1 - \frac{v_0}{u_0+e_2}) = v_1, \end{cases} \tag{4.1}$$

$$\begin{cases} u_1 + u_1(1 - \beta u_1) - \frac{mu_1v_1}{u_1+e_1} = u_2, \\ v_1 + sv_1(1 - \frac{v_1}{u_1+e_2}) = v_2, \end{cases} \tag{4.2}$$

and

$$\begin{cases} u_2 + u_2(1 - \beta u_2) - \frac{mu_2v_2}{u_2+e_1} = \bar{u}, \\ v_2 + sv_2(1 - \frac{v_2}{u_2+e_2}) = \bar{v}. \end{cases} \tag{4.3}$$

If Eqs. (4.1), (4.2) and (4.3) have positive solutions $z_i$, $i = 0, 1, 2$, which are all different from $\bar{z}$, then $F^3$ is constructed to map the point $z_0 = (u_0, v_0)$ to $\bar{z} = (\bar{u}, \bar{v})$ after three iterations. Indeed, from the first equation of Eq. (4.3), it follows that

$$v_2 = \frac{(u_2 + e_1)(u_2 + u_2(1 - \beta u_2) - \bar{u})}{mu_2}. \tag{4.4}$$

Putting it in the second one of Eq. (4.3) gives an equation which $u_2$ satisfies:

$$\begin{aligned} H(u) = {} & -\beta^2 su^6 + \bigl(-2\beta^2 e_1 s - \beta ms - \beta m + 4\beta s\bigr)u^5 + \bigl(-\beta^2 e_1^2 s - \beta e_1 ms - \beta e_2 ms \\ & - \beta e_1 m + 8\beta e_1 s - \beta e_2 m - 2\beta s\bar{u} + 2ms + 2m - 4s\bigr)u^4 + \bigl(-\beta e_1 e_2 ms \\ & + 4\beta e_1^2 s - \beta e_1 e_2 m - 4\beta e_1 s\bar{u} + 2e_1 ms + 2e_2 ms - m^2\bar{v} - ms\bar{u} + 2e_1 m \\ & - 8e_1 s + 2e_2 m - m\bar{u} + 4s\bar{u}\bigr)u^3 + \bigl(-2\beta e_1^2 s\bar{u} + 2e_1e_2 ms - e_1 ms\bar{u} - e_2 m^2\bar{v} \\ & - e_2 ms\bar{u} - 4e_1^2 s + 2e_1e_2 m - e_1 m\bar{u} + 8e_1 s\bar{u} - e_2 m\bar{u} - s\bar{u}^2\bigr)u^2 \\ & + \bigl(-e_1e_2 ms\bar{u} + 4e_1^2 s\bar{u} - e_1e_2 m\bar{u} - 2e_1 s\bar{u}^2\bigr)u - e_1^2 s\bar{u}^2 = 0. \end{aligned} \tag{4.5}$$

Solving Eq. (4.5) gives $u_2$, then putting it in (4.4) gives $v_2$. Thus, we get point $z_2 = (u_2, v_2)$. Similarly, putting $u_2$, $v_2$ in (4.2), we get $z_1 = (u_1, v_1)$ and $z_0 = (u_0, v_0)$ from $z_1 = (u_1, v_1)$ and (4.1). Let $\mathfrak{B} = \Omega_1 \cap \Omega_2 \cap \Omega_3 \neq \emptyset$, if $\mathfrak{B}$ is a non-empty set and a neighborhood of $\bar{z}$, and the solutions of Eqs. (4.1), (4.2) and (4.3) satisfy $z_0$, $z_1$, $z_2 \neq \bar{z}$; $z_0 \in \mathfrak{B}$, $z_1 \notin \mathfrak{B}$, $z_2 \notin \mathfrak{B}$; and $\det(DF(z_k)) \neq 0$ for $k = 0, 1, 2$, then $\bar{z}$ is a snap-back repeller. In this case the model system (1.4) is chaotic in the sense of Marotto.

*Example* 4.1 Marotto's chaos.

Here, diagrams for bifurcation, chaotic attractors and the largest Lyapunov exponents will be drawn to validate our theoretical result using numerical simulation. As we see in Example 3.1, a Neimark–Sacker bifurcation arises as parameter $s$ varies in a neighborhood of $s_1 = 0.09096349222$. Now increase the value of $s$ to be 3. By a tedious numerical calculation and simulations with $\Phi(1) > 0$, $\Phi(-1) > 0$ and $\Phi(0) > 0$ using

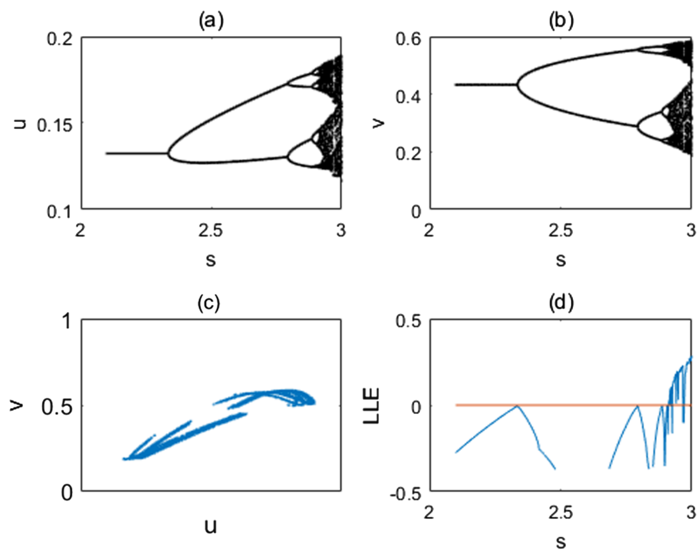


**Figure 5** (**a**) Bifurcation diagram of map (1.4) in the $(s,u)$ plane. (**b**) Bifurcation diagram of map (1.4) in the $(s,v)$ plane. (**c**) Chaotic attractor for $s = 3$. (**d**) The largest Lyapunov exponents corresponding to **a**/**b**

MATLAB software, we find a neighborhood $\mathfrak{B} = \{(u,v) \mid 0 < u < 0.14, 0.25 < v < 0.46\}$ of $E_2$, where all eigenvalues of $DF(z)$ exceed 1 in norm. There also exists a positive point $z_0 = (0.07289604113, 0.2931610206)$ satisfying $F^3(z_0) = E_2$ and $\det(DF(z_k)) = -0.6275618341, -2.100193893, 2.619286018 \neq 0$ for $k = 0,1,2$, respectively. Moreover, $z_0 \in \mathfrak{B}$, $z_1 = (0.09523173812, 0.484637067) \notin \mathfrak{B}$, $z_2 = (0.0817510353, 0.1557479687) \notin \mathfrak{B}$. Thus, $E_2$ is a snap-back repeller.

The Marotto's chaotic attractor is given in Fig. 5(c). The largest Lyapunov exponents (LLE for short) are presented in Fig. 5(d). It can be seen that the largest Lyapunov exponent is positive when $s = 3$, which means that the system is in chaotic state. Incidentally, the system is superstable for some values of $s$ (blank interval in s-axis in Fig. 5(d)), at which the Lyapunov exponents are equal to negative infinity. This is something akin to a critically damped oscillator in that the system heads towards its equilibrium point as quickly as possible [38, 39].

### 4.2 Controlling chaotic dynamical system using an improved OGY method

In this subsection, we apply an improved OGY (Ott, Grebogi and Yorke) method to stabilize the chaotic orbit at the unstable fixed point $E_2$ of model system (1.4), thus achieve the objective of chaos control. The controlled system is given by

$$\begin{pmatrix} u_{n+1} \\ v_{n+1} \end{pmatrix} = \begin{pmatrix} u_n + u_n(1-\beta u_n) - \frac{m u_n v_n}{u_n+e_1} \\ v_n + s v_n(1 - \frac{v_n}{u_n+e_2}) + l, \end{pmatrix}, \tag{4.6}$$

where $l$ is an adjustable, external control parameter. Assume that the system (4.6) is in chaotic state if $l = 0 := l_0$. Obviously, (4.6) possesses a fixed point $E_2$ for $l = l_0$. The linearization of (4.6) near $E_2$ is given by

$$\begin{pmatrix} u_{n+1} - \eta \\ v_{n+1} - (\eta + e_2) \end{pmatrix} = A \begin{pmatrix} u_n - \eta \\ v_n - (\eta + e_2) \end{pmatrix} + G(l - l_0), \tag{4.7}$$

with

$$A = \mathrm{D}_z\overline{F}(l_0, E_2) = \begin{pmatrix} 1 - \beta u^* + \frac{mu^*v^*}{(u^*+e_1)^2} & -\frac{mu^*}{u^*+e_1} \\ s & 1 - s \end{pmatrix},$$

$$G = \mathrm{D}_l\overline{F}(l_0, E_2) = \begin{pmatrix} 0 \\ 1 \end{pmatrix},$$

where

$$\overline{F}(z, l) = \bigl(\overline{F}_1(z, l), \overline{F}_2(z, l)\bigr)^{\mathrm{T}},$$

$$\overline{F}_1(z_n, l) = u_n + u_n(1 - \beta u_n) - \frac{mu_nv_n}{u_n + e_1},$$

$$\overline{F}_2(z_n, l) = v_n + sv_n\left(1 - \frac{v_n}{u_n + e_2}\right) + l.$$

The control law is designed as

$$l - l_0 = -K^{\mathrm{T}}(z_n - E_2) = -k_1(u_n - \eta) - k_2(v_n - \eta - e_2),$$

where $K = (k_1, k_2)^{\mathrm{T}}$ is a state feedback gain matrix. Let $\delta z_n = z_n - E_2$, then system (4.7) becomes

$$\delta z_{n+1} = \bigl(A - GK^{\mathrm{T}}\bigr)\delta z_n. \tag{4.8}$$

We construct a matrix, called the control matrix, as follows:

$$U = (G \mid AG) = \begin{pmatrix} 0 & -\frac{mu^*}{u^*+e_1} \\ 1 & 1 - s \end{pmatrix}.$$

Since $U$ is of full rank, the system (4.8) is controllable. Under this condition, for given matrices $A$ and $G$, $A - GK^{\mathrm{T}}$ can always possesses specified eigenvalues by regulating matrix $K$. Once the absolute values of all eigenvalues are less than 1, one can control system. Define the transformation matrix $\overline{T} = UW$, where

$$W \triangleq \begin{pmatrix} a_1 & 1 \\ 1 & 0 \end{pmatrix},$$

$a_1$ is the $\mu$-term coefficient of characteristic polynomial associated with the matrix $A$, that is,

$$|\mu I - A| = \mu^2 + a_1\mu + a_2 = 0,$$

whereas the expected characteristic equation is

$$\bigl|\rho I - A + GK^{\mathrm{T}}\bigr| = \rho^2 + \alpha_1\rho + \alpha_2 = 0,$$

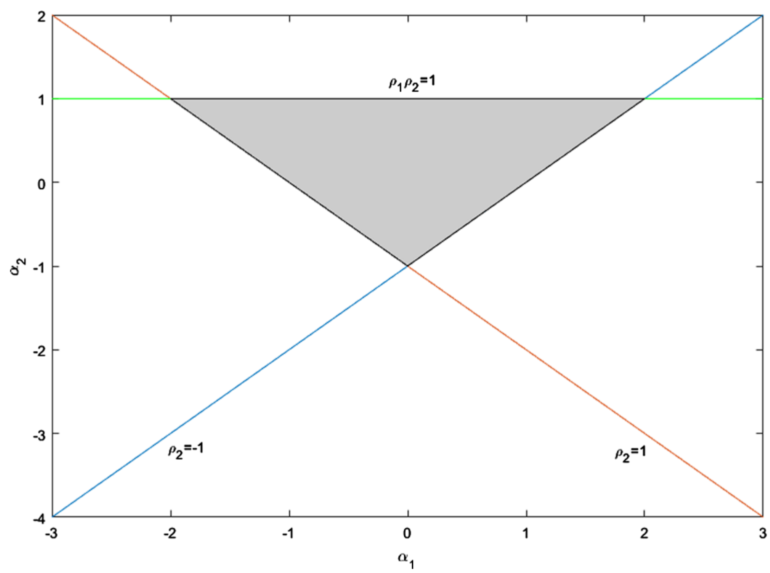


**Figure 6** The stability region of controlled system (4.6) in the $(\alpha_1,\alpha_2)$ plane

with

$$\alpha_1 = -(\rho_1 + \rho_2),$$
$$\alpha_2 = \rho_1\rho_2.$$

The matrix $K$ is determined by the equation below:

$$K^{\mathrm{T}} = (\alpha_2 - a_2, \alpha_1 - a_1)\overline{T}^{-1}. \tag{4.9}$$

Note that we just need $|\rho_i| < 1$, $i = 1,2$ for the purpose of controlling chaos. Thus, $\alpha_1$ and $\alpha_2$ will be allowed to take values from a bounded region (called the stability region; see the triangular region in Fig. 6) in the $(\alpha_1,\alpha_2)$ plane. As a result, $K$ is not unique.

*Example* 4.2 Controlling chaos.

As seen in Example 4.1, the system (1.4) is chaotic when $s = 3$. In the following, we determine the stability region in the $(k_1,k_2)$ plane. With Eq. (4.9) we get

$$\begin{cases} k_1 = -3.5909818769\alpha_1 - 3.35529711721005\alpha_2 - 0.843221746, \\ k_2 = \alpha_1 - 0.929757409. \end{cases} \tag{4.10}$$

Then from (4.10) and the ranges for $\alpha_1$, $\alpha_2$, we obtain the stability region (see Fig. 7), surrounded by three lines:

$$L_1: -0.2980361992k_1 - 2.07024259k_2 - 1.176133991 = 0.$$
$$L_2: -0.2980361992k_1 - 0.07024259k_2 + 0.683380827 = 0,$$
$$L_3: -0.2980361992k_1 - 1.07024259k_2 - 2.246376582 = 0.$$

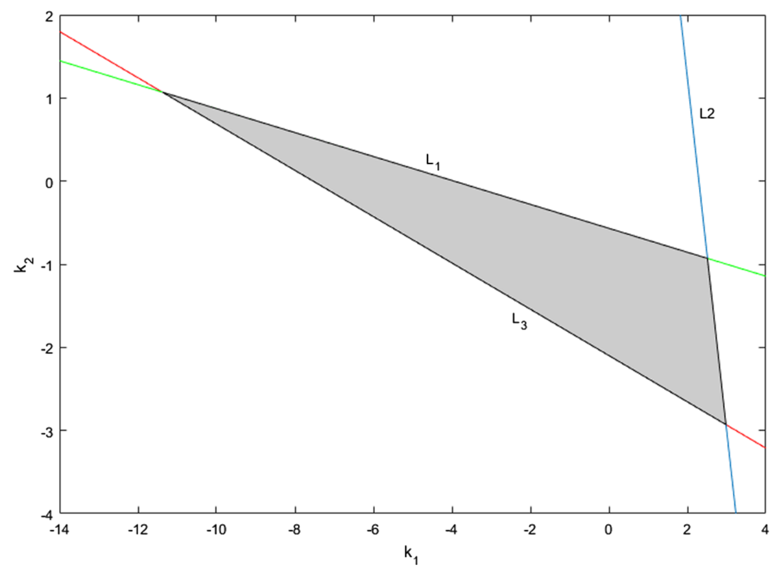


**Figure 7** The stability region of controlled system (4.6) in the $(k_1, k_2)$ plane for $s = 3$, $m = 3$, $\beta = 0.2$, $e_1 = 1.2$, $e_2 = 0.3$

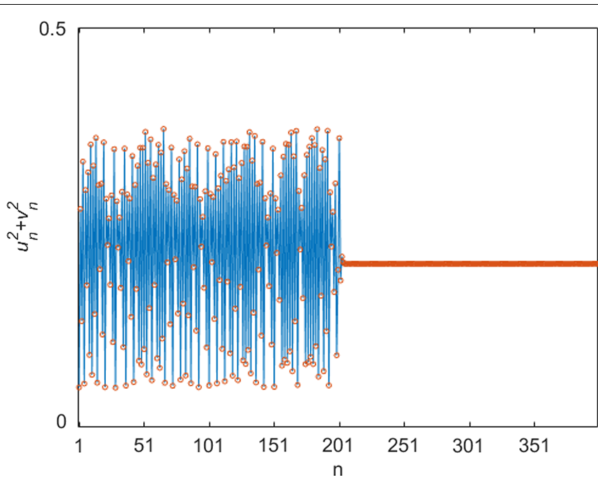


**Figure 8** Time series data for controlled system (4.6) for $s = 3$, $m = 3$, $\beta = 0.2$, $e_1 = 1.2$, $e_2 = 0.3$, $k_1 = -0.843221746$ and $k_2 = -0.929757409$. The initial value is $(0.1, 0.2)$ and the control is activated after the 200th iteration

We let initial value as $(0.1, 0.2)$, and take $k_1 = -0.843221746$, $k_2 = -0.929757409$ from the stability region. The control result is shown in Fig. 8. We can see that the chaotic orbits enter the controllable region when $n > 200$, and it is shown that the chaotic trajectory is stabilized.

## 5 Conclusion

The present paper is concerned with the dynamical behavior and control of a discrete-time predator–prey system with modified Leslie–Gower and Holling's type II schemes. We have seen that our results show far richer dynamics of the discrete model compared with the continuous one, including invariant circle, superstable phenomenon, cascades of period-doubling bifurcation and chaotic sets. In the meantime, these results demonstrate that the natural growth rates of predator and prey play a vital role for local and global stability of predator–prey system. It indicates that the dynamical behavior of biological model may be very sensitive to bifurcation parameter perturbation. Especially, we provide the method of state feedback and parameter perturbation for bifurcation control, and the improved OGY method for chaos control, which stabilize the chaotic orbit at an unstable fixed point. Numerical simulations are carried out to verify our theoretical analysis and control strategies. Our results can be useful for the specialists in organic agriculture as they need a biological control method. However, it is still a challenging problem to explore the multiple-parameter bifurcation in biological systems. But at present the study in this respect is very inadequate. This will be the topic of our future research and we expect to obtain some more analytical results.

**Acknowledgements**
The authors wish to express their gratitude to the editors and reviewers for the helpful comments.

**Funding**
This research is supported by National Natural Science Foundation of China under grant No. 71271158.

**Competing interests**
The authors declare that they have no competing interests.

**Authors' contributions**
The study presented here was carried out in collaboration between both authors. Both authors read and approved the final manuscript.

**Authors' information**
Dr. Donghan Cai is a professor at the Wuhan University School of Mathematics and Statistics, Bayi Road, Wuhan City, Hubei Province, China. E-mail: dhcai@whu.edu.cn.

## Publisher's Note
Springer Nature remains neutral with regard to jurisdictional claims in published maps and institutional affiliations.

Received: 1 September 2018 Accepted: 7 January 2019 Published online: 17 January 2019

**References**
1. Edelstein-Keshet, L.: Mathematical Models in Biology. Random House, New York (1988)
2. Leslie, P.H., Gower, J.C.: The properties of a stochastic model for the predator–prey type of interaction between two species. Biometrika **47**(3–4), 219–234 (1960)
3. Aziz-Alaoui, M.A., Daher Okiye, M.: Boundedness and global stability for a predator–prey model with modified Leslie–Gower and Holling-type II schemes. Appl. Math. Lett. **16**(7), 1069–1075 (2003)
4. Kolmogorov, A.N.: Sulla teoria di Volterra della Lotta per l'esistenza. G. Ist. Ital. Attuari **7**, 74–80 (1936) (in Italian)
5. Wei, C.J., Liu, J.N., Zhang, S.W.: Analysis of a stochastic eco-epidemiological model with modified Leslie–Gower functional response. Adv. Differ. Equ. **2018**, 119 (2018). https://doi.org/10.1186/s13662-018-1540-z
6. Aziz-Alaoui, M.A.: Study of a Leslie–Gower-type tritrophic population model. Chaos Solitons Fractals **14**(8), 1275–1293 (2002)
7. Liang, Z.Q., Pan, H.W.: Qualitative analysis of a ratio-dependent Holling–Tanner model. J. Math. Anal. Appl. **334**(2), 954–964 (2007)
8. Yang, W.S.: Global asymptotical stability and persistent property for a diffusive predator–prey system with modified Leslie–Gower functional response. Nonlinear Anal., Real World Appl. **14**(3), 1323–1330 (2013)
9. Peng, R., Wang, M.X.: Global stability of the equilibrium of a diffusive Holling–Tanner prey-predator model. Appl. Math. Lett. **20**(6), 664–670 (2007)
10. Nindjin, A.F., Tia, K.T., Okou, H., Tetchi, A.: Stability of a diffusive predator–prey model with modified Leslie–Gower and Holling-type II schemes and time-delay in two dimensions. Adv. Differ. Equ. **2018**, 177 (2018). https://doi.org/10.1186/s13662-018-1621-z
11. Banerjee, C., Das, P.: Impulsive effect on Tri-Trophic food chain model with mixed functional responses under seasonal perturbations. Differ. Equ. Dyn. Syst. **26**(1–3), 157–176 (2018)
12. Xu, Y., Liu, M., Yang, Y.: Analysis of a stochastic two-predators one-prey system with modified Leslie–Gower and Holling-type II schemes. J. Appl. Anal. Comput. **7**(2), 713–727 (2017)
13. Degn, H., Holden, A.V., Olsen, L.F.: Chaos in Biological Systems. Springer, New York (1987)
14. Bai, Y.Z., Mu, X.Q.: Global asymptotic stability of a generalized SIRS epidemic model with transfer from infectious to susceptible. J. Appl. Anal. Comput. **8**(2), 402–412 (2018)

15. Han, M.A., Sheng, L.J., Zhang, X.: Bifurcation theory for finitely smooth planar autonomous differential systems. J. Differ. Equ. **264**(5), 3596–3618 (2018)
16. Romanovski, V.G., Han, M.A., Huang, W.T.: Bifurcation of critical periods of a quintic system. Electron. J. Differ. Equ. **2018**, 66 (2018)
17. Li, M.M., Wang, J.R.: Exploring delayed Mittag-Leffler type matrix functions to study finite time stability of fractional delay differential equations. Appl. Math. Comput. **324**, 254–265 (2018)
18. Cao, X.K., Wang, J.R.: Finite-time stability of a class of oscillating systems with two delays. Math. Methods Appl. Sci. **41**(13), 4943–4954 (2018)
19. Zhang, X., Zhang, Q.L.: Bifurcation analysis and control of a discrete harvested prey-predator system with Beddington–DeAngelis functional response. J. Franklin Inst. **347**(7), 1076–1096 (2010)
20. Zhang, H.Y., Ma, S.N., Huang, T.S., Cong, X.B., Gao, Z.C., Zhang, F.F.: Complex dynamics on the routes to chaos in a discrete predator–prey system with Crowley–Martin type functional response. Discrete Dyn. Nat. Soc. **2018** (2018). https://doi.org/10.1155/2018/2386954
21. Baek, H.: Complex dynamics of a discrete-time predator–prey system with Ivlev functional response. Math. Probl. Eng. **2018** (2018). https://doi.org/10.1155/2018/8635937
22. Wu, D.Y., Zhao, H.Y.: Complex dynamics of a discrete predator–prey model with the prey subject to the Allee effect. J. Differ. Equ. Appl. **23**(11), 1765–1806 (2017)
23. Hu, Z.Y., Teng, Z.D., Zhang, L.: Stability and bifurcation analysis of a discrete predator–prey model with nonmonotonic functional response. Nonlinear Anal., Real World Appl. **12**(4), 2356–2377 (2011)
24. Alligood, K., Sauer, T., Yorke, J.: Chaos: An Introduction to Dynamical System. Springer, New York (1997)
25. Guckenheimer, J., Holmes, P.: Nonlinear Oscillations, Dynamical Systems, and Bifurcations of Vector Fields. Springer, New York (2002)
26. He, Z.M., Lai, X.: Bifurcation and chaotic behavior of a discrete-time predator–prey system. Nonlinear Anal., Real World Appl. **12**(1), 403–417 (2011)
27. Wiggins, S.: Introduction to Applied Nonlinear Dynamical System and Chaos. Springer, New York (2003)
28. Chen, Z., Yu, P.: Controlling and anti-controlling Hopf bifurcations in discrete maps using polynomial functions. J. Franklin Inst. **26**(4), 1231–1248 (2005)
29. Elabbasy, E.M., Agiza, H.N., El-Metwally, H., Dlsadany, A.A.: Bifurcation analysis, chaos and control in the Burgers mapping. Int. J. Nonlinear Sci. **4**(3), 171–185 (2007)
30. Luo, X.S., Chen, G.R., El-Metwally, B.H.: Hybrid control of period-doubling bifurcation and chaos in discrete nonlinear dynamical system. Chaos Solitons Fractals **18**(4), 775–783 (2003)
31. Hawkins, B.A., Cornell, H.V.: Theoretical Approaches to Biological Control. Cambridge University Press, Cambridge (2004)
32. Gopalsamy, K., Weng, P.: Feedback regulation of logistic growth. Int. J. Math. Math. Sci. **16**(1), 177–192 (1993)
33. Marotto, F.R.: Snap-back repellers imply chaos in $\mathbb{R}^n$. J. Math. Anal. Appl. **63**(1), 199–223 (1978)
34. Marotto, F.R.: On redefining a snap-back repeller. Chaos Solitons Fractals **25**(1), 25–28 (2005)
35. Liao, K.L., Shih, C.W.: Snapback repellers and homoclinic orbits for multi-dimensional maps. J. Math. Anal. Appl. **386**(1), 387–400 (2012)
36. Yuan, S.L., Jing, Z.J., Jiang, T.: Bifurcation and chaos in the Tinkerbell map. Int. J. Bifurc. Chaos Appl. Sci. Eng. **21**(11), 3137–3156 (2011)
37. Ren, J.L., Siegmund, S.: Bifurcations and chaos in a discrete predator–prey model with Crowley–Martin functional response. Nonlinear Dyn. **90**(1), 19–41 (2017)
38. Arrowsmith, D.K., Cartwright, J.H.E., Lansbury, A.N., Place, C.M.: The Bogdanov map: bifurcations, mode locking, and chaos in a dissipative system. Int. J. Bifurc. Chaos **3**(4), 803–842 (1993)
39. Gu, Q.L.L., Tian, Z.Q.K., Kovacic, G., Zhou, D., Cai, D.: The dynamics of balanced spiking neuronal networks under Poisson drive is not chaotic. Front. Comput. Neurosci. **12**, 47 (2018) https://doi.org/10.3389/fncom.2018.00047